JGR Space Physics

RESEARCH ARTICLE
10.1029/2019JA026884

Special Section:
Long-term changes and Trends in the Middle and Upper Atmosphere

Pedersen Ionic Contribution in Different Time Scales

Bruno S. Zossi[1,2], Mariano Fagre[2,3], and Ana G. Elias[1,2]

[1]Laboratorio de Fisica de la Atmosfera, INFINOA (CONICET-UNT), Facultad de Ciencias Exactas y Tecnologia, Universidad Nacional de Tucuman, San Miguel de Tucumán, Argentina, [2]Consejo Nacional de Investigaciones Cientificas y Tecnicas, CONICET, Buenos Aires, Argentina, [3]Laboratorio de Telecomunicaciones, Departamento de Electricidad, Electrónica y Computación, Facultad de Ciencias Exactas y Tecnología, Universidad Nacional de Tucuman, San Miguel de Tucumán, Argentina

Key Points:
- Pedersen conductance calculation on different time scales
- Ionic contribution to Pedersen conductance considering days, months, and years

Correspondence to:
B. S. Zossi,
brunozossi@hotmail.com

Citation:
Zossi, B. S., Fagre, M., & Elias, A. G. (2019). Pedersen ionic contribution in different time scales. *Journal of Geophysical Research: Space Physics*, *124*. https://doi.org/10.1029/2019JA026884

Received 26 APR 2019
Accepted 22 JUN 2019
Accepted article online 30 JUN 2019

Abstract Pedersen conductivity is one of the main parameters in atmospheric electrodynamics, magnetosphere-ionosphere-thermosphere coupling, and several other geophysical processes. It is determined by the collision frequency between charged and neutral components and the Earth's magnetic field intensity through the gyrofrequency. This work analyzes the contribution of different ionic species to the variability of Pedersen conductance in time scales from hours to years within the period 1964–2008 based on the results of various atmospheric and ionospheric models. The main results are (1) there is a positive correlation between O^+ density and Pedersen conductance, (2) Pedersen conductance of *F* layer has a larger increase with the solar activity than that of *E* layer, (3) Pedersen conductance has a long-term trend that is determined by Earth's magnetic field intensity and electron density, and (4) at midlatitudes trends are mainly governed by the Earth's magnetic field and modulated by the electron density, while at high latitudes both are important.

1. Introduction

The ionosphere is a conducting medium due to the presence of free charges: ions and electrons. The conductivity σ in this case is a tensor due to the Earth's magnetic field, which acts as an applied external field turning the ionosphere into an anisotropic medium. The σ is given by Rishbeth and Garriott (1969) and Schunk and Nagy (2009).

$$\sigma = \begin{pmatrix} \sigma_1 & -\sigma_2 & 0 \\ \sigma_2 & \sigma_1 & 0 \\ 0 & 0 & \sigma_o \end{pmatrix} \tag{1}$$

where σ_1 and σ_2 are the Pedersen and Hall conductivities, respectively, both oriented perpendicular to magnetic field, and σ_o is the parallel conductivity defined along the magnetic field. These conductivities' equations are (Moen & Brekke, 1990; Rishbeth & Garriott, 1969; Schunk & Nagy, 2009; Takeda & Araki, 1985)

$$\sigma_0 = N_e e^2 \left[\frac{1}{m_e \nu_e} + \sum_i \frac{f_i}{m_i \nu_i} \right] \tag{2}$$

$$\sigma_1 = N_e e^2 \left[\frac{1}{m_e} \cdot \frac{\nu_e}{(\nu_{e^2} + \omega_{e^2})} + \sum_i \frac{f_i}{m_i} \cdot \frac{\nu_i}{(\nu_{i^2} + \omega_{i^2})} \right] \tag{3}$$

$$\sigma_2 = N_e e^2 \left[\frac{1}{m_e} \cdot \frac{\omega_e}{(\nu_{e^2} + \omega_{e^2})} - \sum_i \frac{f_i}{m_i} \cdot \frac{\omega_i}{(\nu_{i^2} + \omega_{i^2})} \right] \tag{4}$$

subscripts *e* and *i* stand for electron and ions respectively, N_e is the electron density, *m* the mass, *e* the electron charge, ν the collision frequency, ω = eB/m the gyrofrequency, *B* the Earth's magnetic field intensity, and *f* the relative density of each ion species. Plasma neutrality and single positive charged ion species are assumed. The main conducting ions in the ionosphere are nitric oxide (NO^+), molecular oxygen (O_2^+), and atomic oxygen (O^+).

Collision frequencies of charged particles, as is usual in the ionosphere, are considered only as collisions with neutral species, so electron and ions collision frequency are considered $\nu_e = \nu_{en}$ and $\nu_i = \nu_{in}$,

©2019. American Geophysical Union. All Rights Reserved.

respectively (Rishbeth & Garriott, 1969). In fact, at the height where conductivities are maximum the electron-ion and ion-electron collisions are negligible.

Pedersen conductivity maximum occurs near 120 km. Ionic species contributes in different quantities to the total conductivity, and each ionic contribution has a different peak height. Pedersen conductance, Σ_1, that is the height integrated conductivity

$$\Sigma_1 = \int_{z_1}^{z_2} \sigma_1 \, dz \tag{5}$$

where z_1 and z_2 are the bottom and top of the ionosphere, respectively, presents different contributions from each conducting ion type.

Previous studies of ionospheric conductance variability do not analyze the contribution of each ion species separately. However, there are some works that discriminate between atomic and molecular species providing some insight into their different contributions.

Rasmussen et al. (1988) pointed out that for maximum solar activity levels the contribution to Hall and Pedersen conductances from the *F* region above 170 km could reach 40% during daytime hours and 80% during night. While during minimum levels this percentage goes down to 20%. This *F* region contribution implies mainly O^+ conductance, since above this level it is the main ion species.

Brekke and Hall (1988) in a study of Hall and Pedersen conductivities and conductances for a quiet summer auroral ionosphere analyze first the effect of collision frequency models on the conductivity profiles and conductances by comparing two different sets of expressions. The main effect is shifting the conductivity peak height by a few kilometers. They consider two ion species with masses 16 and 30.5 in atomic mass units, respectively, corresponding to atomic oxygen and a pseudo molecular species that consists in a mixture of 75% NO^+ and 25% $O_2{}^+$. They analyze then conductances daily variation, assuming a dependence on a linear combination of two cosine of the zenith solar angle. In the case of Pedersen conductance they obtain similar contributions from both terms, which would mean that the *F* region can have a similar contribution than the *E* region, pointing out the importance of O^+ species (the principal ion in the *F* region) also as a conducting ion.

Moen and Brekke (1990) analyze the effects on Hall and Pedersen conductances of two different ion composition models during solar minimum conditions. They found a negligible difference between them concluding that there is a small contribution to the height integrated conductivities from the height region where the variation in ion composition is iomportant, that is above ~170 km. They also conclude that conductivities are well represented considering a single ion species, which they call pseudo-ion, of mass 30.5 (mixture of 75% NO^+ and 25% $O_2{}^+$), as in Brekke and Hall (1988).

Sheng et al. (2017) studied the relation of *E* to *F* layer conductances in order of estimate the coupling of these layers on different solar and geomagnetic activity scenarios.

These works are among the few that study ionospheric conductivities and conductances considering different ions. But none of them show the variation of the contribution of each ion to the total conductance. A first attempt is done by Zossi et al. (2018) studying the role of the three main ions, NO^+, $O_2{}^+$, and O^+, in Pedersen conductivity height profile and in the conductance global pattern for different solar activity levels and seasons. They observe that NO^+ is the main contributor for the maximum conductivity in all the cases in the *E* layer; however, O^+ takes relevance at certain regions such as the South Atlantic Anomaly, where the Earth's magnetic field is depressed, and the crests at the equatorial ionization anomaly (EIA), where the *F* region ionization is enhanced, becoming the main conducting ion in these zones when the solar activity is high.

Regarding Pedersen conductance long-term trends, two sources can be highlighted: secular variations of the Earth's magnetic field, which directly affects the gyrofrequency, and the increasing greenhouse gases concentration that cools the upper atmosphere inducing a contraction of the thermosphere with consequent changes in electron and ion concentrations.

Extrapolating Rishbeth and Roble (1992) predictions for a doubling CO_2 scenario to real values, an foE increase of ~1.2×10^{-3} MHz per decade should be expected. Elias et al. (2010), analyzing long-term trends in the quiet geomagnetic field variation, *Sq*, directly linked to ionospheric conductance, argue that, since the

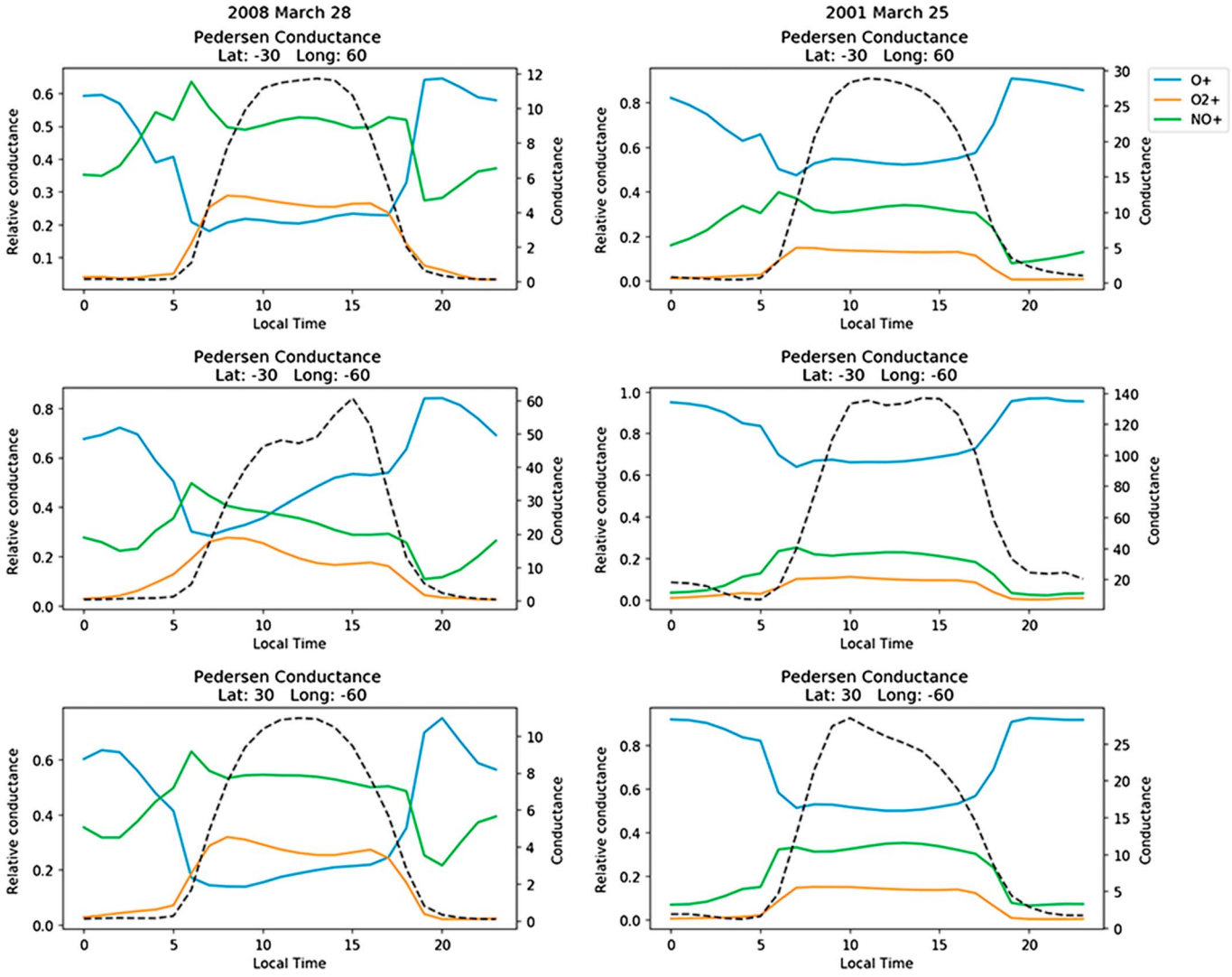

Figure 1. Pedersen conductance in siemens (black dashed line) and ionic contribution (blue = O^+, green = NO^+, and orange = O_2^+) in terms of local time for low (2008, left column) and high solar (2001, right column) activity levels, at three midlatitude locations: 30°S 60°E (top row), 30°S 60°W at the South Atlantic Magnetic Anomaly (middle row), and 30°N 60°W (bottom row).

major part of the Pedersen conductance is in the *E* region, this same increase should be expeced in conductance worldwide.

Cnossen et al. (2011) analyze changes in the spatial distribution of ionospheric conductance due to magnetic field changes using the Coupled Magnetosphere-Ionosphere-Thermosphere model. They considered a decrease in the Earth's internal magnetic field modeling it as a centered dipole and clearly observed conductances increase with the greatest variations during daytime hours. In a later work by Cnossen et al. (2012), a larger range of dipole moments was considered together with different solar activity level conditions, showing in this case the global mean conductance. Cnossen and Richmond (2012), with the same model, analyzed the variation of Hall and Pedersen conductances integrated over high magnetic latitudes, due to changes in the dipole tilt angle between 0° and 60°. Their results show that these conductances are larger when the magnetic pole of the hemisphere in question is tilted more toward the Sun.

Zossi et al. (2018) go further in time and analyze conductances variation expected during several Earth's magnetic field reversal scenarios, considering extremely weak and much less uniform fields. In addition to a global conductance increase, the spatial gradient becomes stronger at some regions.

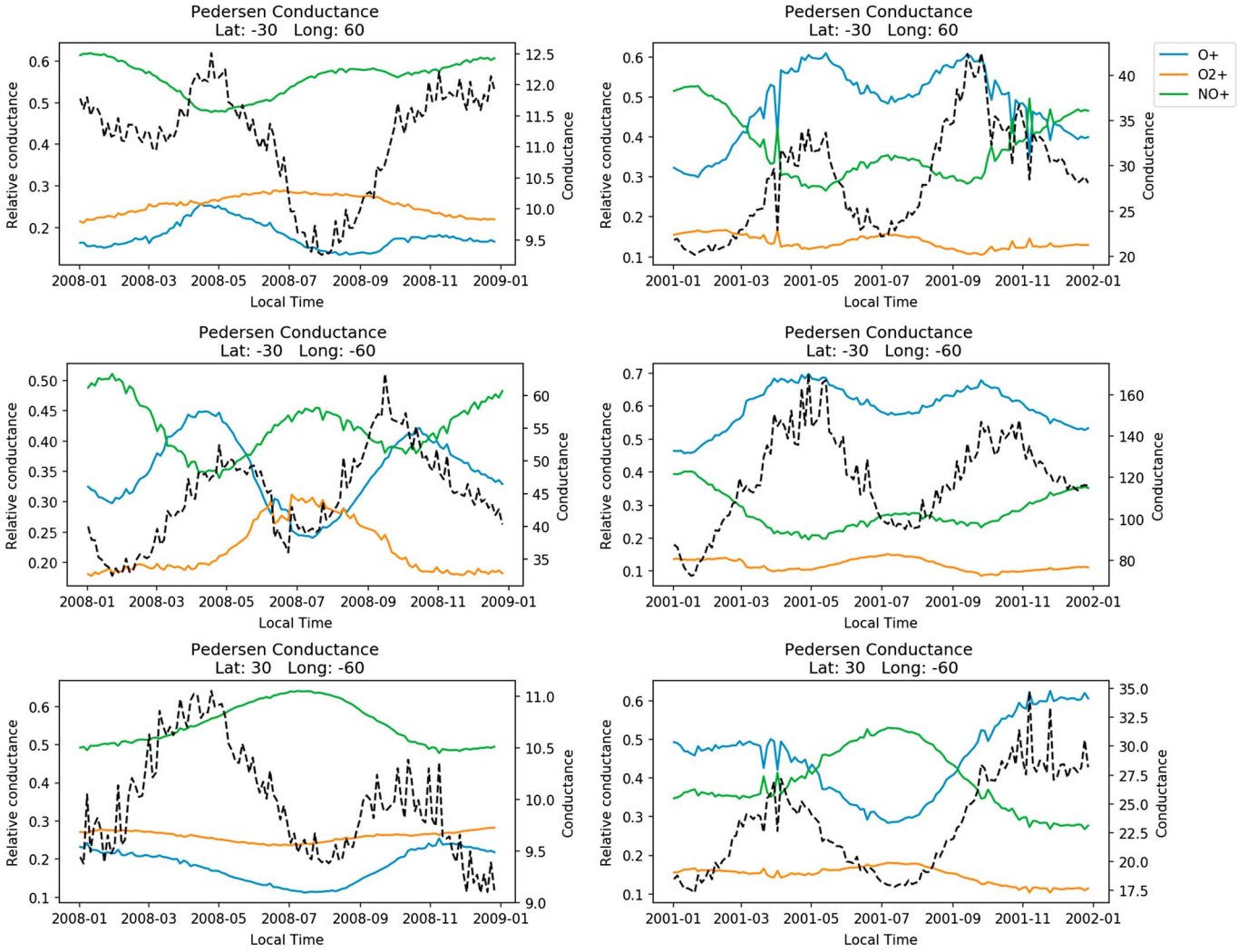

Figure 2. Pedersen conductance in siemens (black dashed line) and ionic contribution (blue = O^+, green = NO^+, and orange = $O_2{}^+$) during solar minimum and maximum (2008 and 2001), for three locations: 30°S 60°E (top row), 30°S 60°W (middle row, South Atlantic Magnetic Anomaly), and 30°N 60°W (bottom row). Conductance was calculated for 12 LT.

Ionic global spatial distribution of Pedersen conductance is evaluated on different seasons and solar activity levels by Zossi, Fagre, and Elias (2018). They show that O^+ take bigger percentages of conductance in regions like the EIA and South Atlantic Magnetic Anomaly (SAA) and becomes almost the main conducting ion under high solar activity level.

In this work the contribution of each main conducting ion species to Pedersen conductance and its variation are analyzed considering time scales from daily to long-term trends during a 44-year period between 1964 and 2008.

2. Methodology

Pedersen conductivity of each ion species can be separately calculated as

$$\sigma_{1i} = \frac{N_i\, e^2}{m_i} \cdot \frac{\nu_i}{(\nu_{i^2} + \omega_{i^2})} \tag{6}$$

and the integrated conductivity is calculated as a finite sum

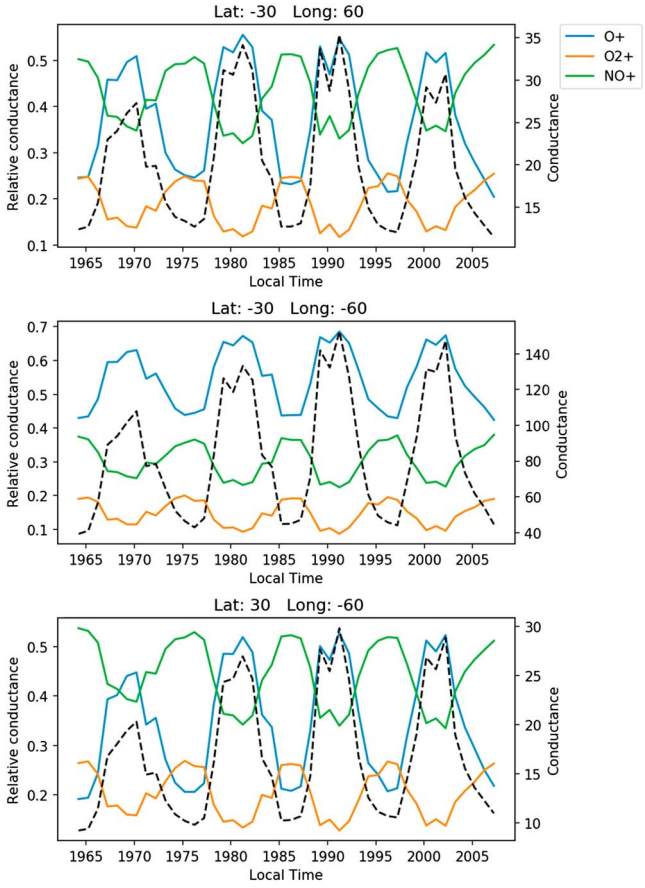

Figure 3. Pedersen conductance in siemens (black dashed line) and ionic contribution (blue = O^+, green = NO^+, and orange = O_2^+) during period 1964 and 2008, taking three positions on Earth, 30°S 60°E (top), 30°S 60°W (middle, South Atlantic Magnetic Anomaly), and 30°N 60°W (bottom). Conductance was calculated for 12 LT.

$$\Sigma_{1i} = \sum_{z_1}^{z_2} \sigma_{1i}\, \Delta z \tag{7}$$

where N_i is the number density of ion i, which stands for NO^+, O_2^+, and O^+, z_1 and z_2 is set to 80 and 500 km, respectively, and a step Δz of 5 km, smaller than scale height in ionosphere. The three most abundant ionospheric ion species in the range 80–500 km were considered: NO^+, O^+, and O_2^+. Collision frequencies with O_2, O, and N_2 are included since they are the most abundant neutral components at the heights here involved.

Collision frequencies for each type of collision were calculated from the equations used by the Thermosphere Ionosphere Electrodynamic General Circulation Model (High Altitude Observatory, 2017; Schunk & Nagy, 2009). N_i for each ions species, N_e, and temperatures were obtained from the International Reference Ionosphere, IRI-2012 (Bilitza et al., 2014), while densities of neutral components from the NRLMSISE-00 empirical atmospheric model (Picone et al., 2002). The magnetic field was obtained from IGRF12 (Thébault et al., 2015).

The variables that play a key role in equation (6) are the electron density and the magnetic field through the gyrofrequency, which in turn vary with location. Five particular locations were selected for this study. Three are at midlatitudes: 30°S 60°E, 30°S 60°W, and 30°N 60°W, and two at high latitude, within the polar region: 75°N 60°E and 75°S 60°E. The midlatitude stations are located out of the EIA region with different variation patterns of the Earth's magnetic field: increasing intensity at 30°S 60°E; SAA region at 30°S 60°W; and decreasing intensity at 30°N 60°W.

Minimum and maximum solar activity levels were evaluated for the solar cycle variation analysis considering 2008 and 2001, respectively.

3. Results and Discussion

Geographic polar areas have a different behavior than midlatitudes, not only for the proximity to the magnetic poles but also for the big solar angle of incoming radiation, so we make a separate analysis for these areas.

3.1. Midlatitudes

Figure 1 shows the daily variation of Σ_1 and of each relative ionic contribution for low and high solar activity levels at the three midlatitude locations. NO^+ contribution presents the expected daily variation with a marked decrease during nighttime. This is due to the decrease of ionization during night at the *E* layer. The same happens to O_2^+ that has its peak value at heights even lower than NO^+. Instead, O^+ presents the greatest contribution during night, in all the cases, since at the *F* layer, the diminution in the electron density is weaker compared to the lower ionospheric layers, and overcome the effect of a low collision frequency. In fact, Pedersen conductivity at the *F* layer becomes larger than that of the *E* layer at night, taking into account that the conductance is reduced several times in absolute values.

During minimum solar activity level and daytime hours, NO^+ is the main conducting ion except at the SAA region. Here the minimum of *B* raises the peak conductivity layer and make the O^+ contribution larger than NO^+ and O_2^+, as discussed in Zossi, Fagre, and Elias (2018) where conductivity height profiles over SAA are presented at noon.

For high solar activity level, O^+ is the main conducting ion during the whole day in all cases. This is almost a general rule at magnetic midlatitudes, but not for low magnetic latitudes and near to magnetic poles Zossi, Fagre, and Elias (2018). The atomic oxygen role during high solar activity time was also discussed in Zossi, Fagre, and Elias (2018), where the height profile shows how the O^+ has a wide conductivity layer, reaching high percentages of conductance around the world and becoming the main conducting ion in many places.

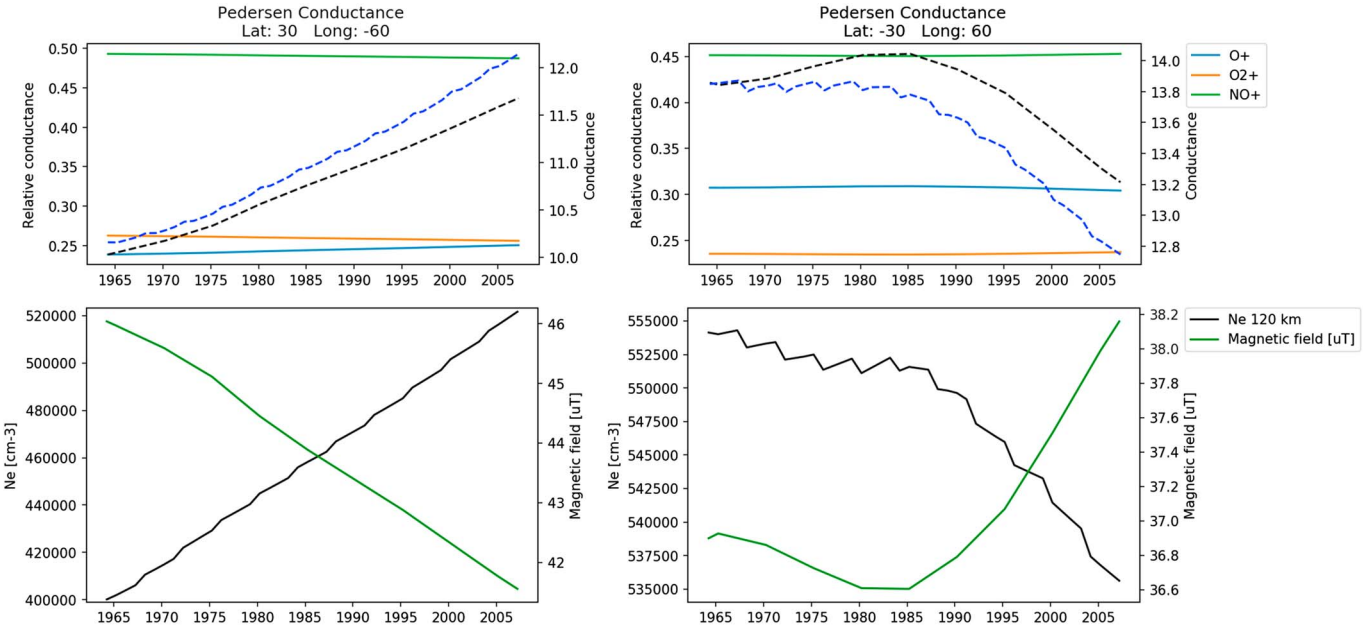

Figure 4. (top row) Pedersen conductance in siemens during period 1964–2008 at two positions: 30°S 60°E (left column) and 30°N 60°W (right column), for an equinoctial month. International Reference Ionosphere /MSIS fixed at 1964 (black dashed line) and International Reference Ionosphere/MSIS with forced to run with low solar activity (blue dashed line). And electron density at 120 km (black) and magnetic field intensity (green) in bottom panels for same locations. MSIS = mass spectrometer and incoherent scatter radar.

Annual variation was analyzed considering 12 LT. Figure 2 shows the annual behavior of Σ_1 and of each ionic contribution. Σ_1 presents semiannual variation at both southern midlatitude locations during solar maximum, determined by the O^+ behavior. At solar minimum the eastern location presents the regular annual variation, with summer values greater than winter with some evidence of a semiannual variation. The western location presents semiannual variation with some evidence of winter anomaly (note that during winter Σ_1 is on average greater than during summer). For the northern location, a combination of winter and semiannual anomaly can be noticed.

In order to analyze solar activity dependence, Figure 3 presents the 44-year period covering 1964–2008 considering equinox period at 12 LT. Σ_1 presents a direct association with solar activity, as expected. A direct

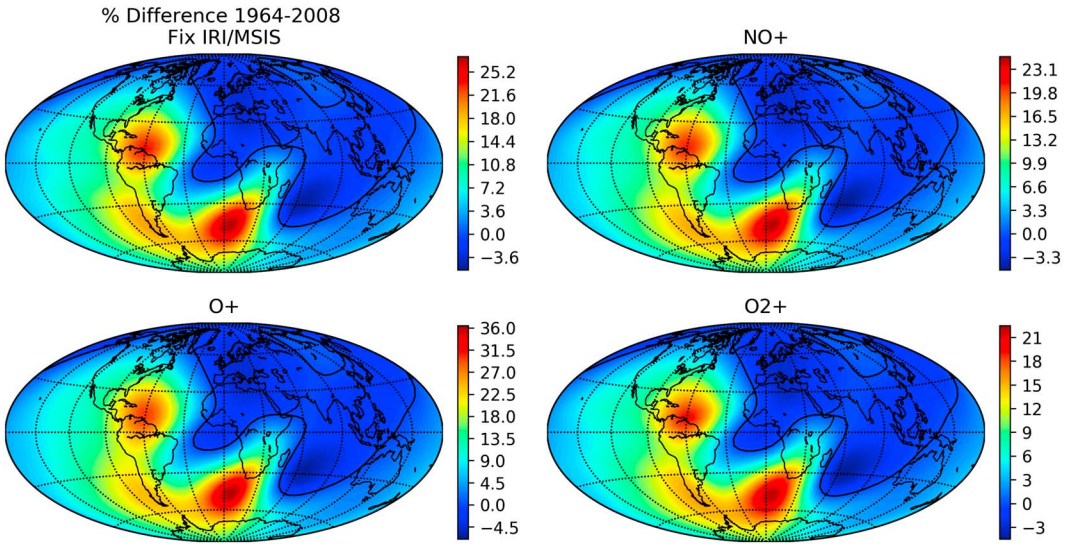

Figure 5. Conductance percentage change between 2008 and 1964 (top left) due only to magnetic field intensity variation and ion contribution variation. Black lines indicate 0% in all panels. IRI = International Reference Ionosphere. MSIS = mass spectrometer and incoherent scatter radar.

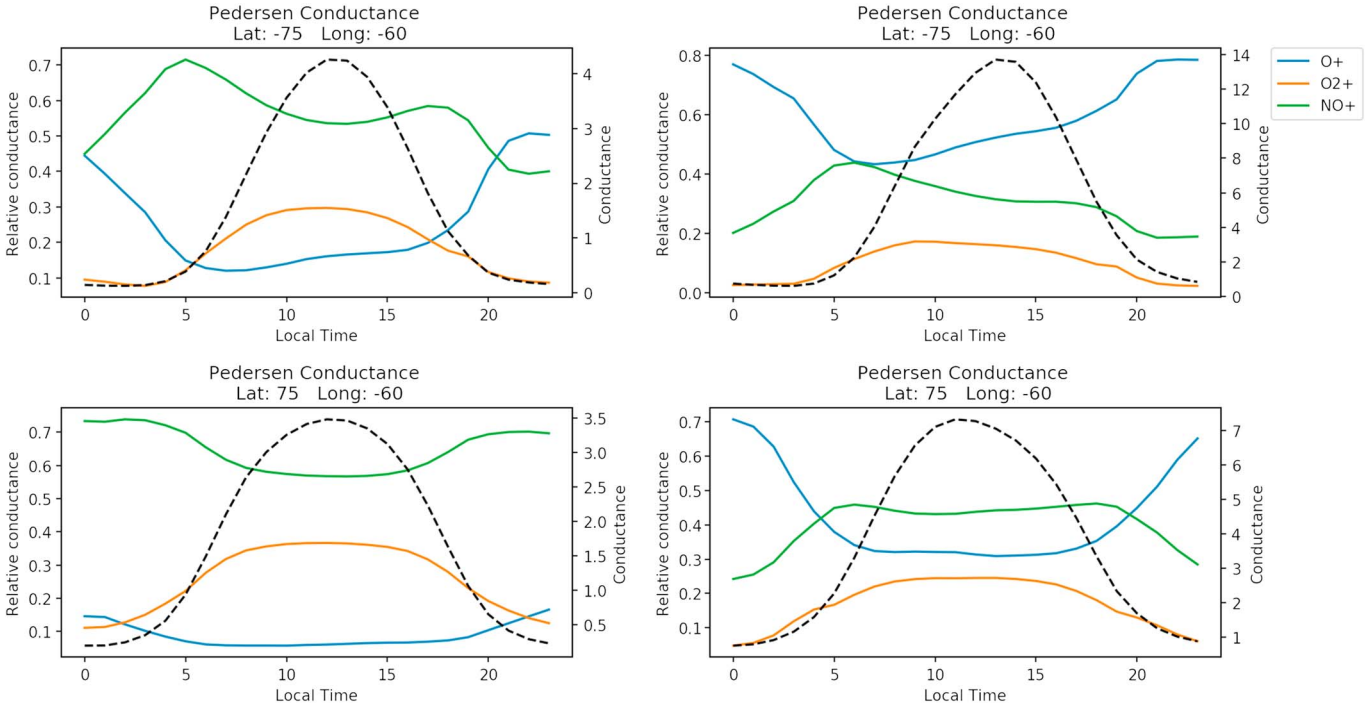

Figure 6. Pedersen conductance in siemens (black dashed line) and ionic contribution (blue = O^+, green = NO^+, and orange = $O_2{}^+$) in terms of local time for low (2008, left column) and high solar (2001, right column) activity levels, at two high-latitude locations: 75°S 60°W (top row) and 75°N 60°W (bottom row).

relation between high solar activity and dominance of O^+ conductance over NO^+ and $O_2{}^+$ is also observed. This result, already obtained by Zossi, Fagre, and Elias (2018), is due to the much stronger response to solar activity variation of the *F*2 region than that of the *E* region. The dependence with the magnetic field can be also noticed in the middle panel of Figure 3, which corresponds to a location within the SAA, where O^+ is the main contributor to Pedersen conductance for every solar activity level. It is possible to estimate a trend using the minimum values. The bottom panel of Figure 3 has a clear increasing behavior, while in the case shown in the top panel there is a decreasing trend along the last four minimums.

For a deep understanding of the decreasing trend during the last four minimums we estimate long-term trends and, for this, solar activity must be filtered out. One way to do this is to fix solar activity level in the models used to obtain the input parameters in the conductances' equations. Another approach is to fix the date in IRI and MSIS (mass spectrometer and incoherent scatter radar) and in this way fixing the solar activity conditions but just changing the magnetic field input. Figure 4 shows both cases, where we can see that the conductance trend response is the inverse to the magnetic field, as expected. The difference between the two methods (black and blue lines) is explained by the electron density trend, which is shown at 120 km in the bottom row of Figure 4 (black line). We can explain the changes in Pedersen conductance only using trends of electron density and magnetic field intensity. In left top panel is also clear that atomic oxygen role increase for a conductance growth.

Now, in order to analyze the magnetic field effect at global scale we made a grid of 5° × 5° latitude-longitude resolution with fixed date. In Figure 5, since the ionosphere and neutral atmosphere are totally fixed, the trends observed can be considered as due only to the Earth's magnetic field variation.

The scales presented in Figure 5 confirm again that the increasing of O^+ conductance is bigger than the other ions even without considering any trend of electron density (since IRI date was fixed).

3.2. Polar Latitudes

The polar areas have a lower Pedersen conductivity than at midlatitudes. The proximity to magnetic poles increase the intensity of magnetic field, and the almost horizontal angle of solar radiation reduces the rate of ion production. These two physical characteristics keep the poles with lower conductivity compared with other places.

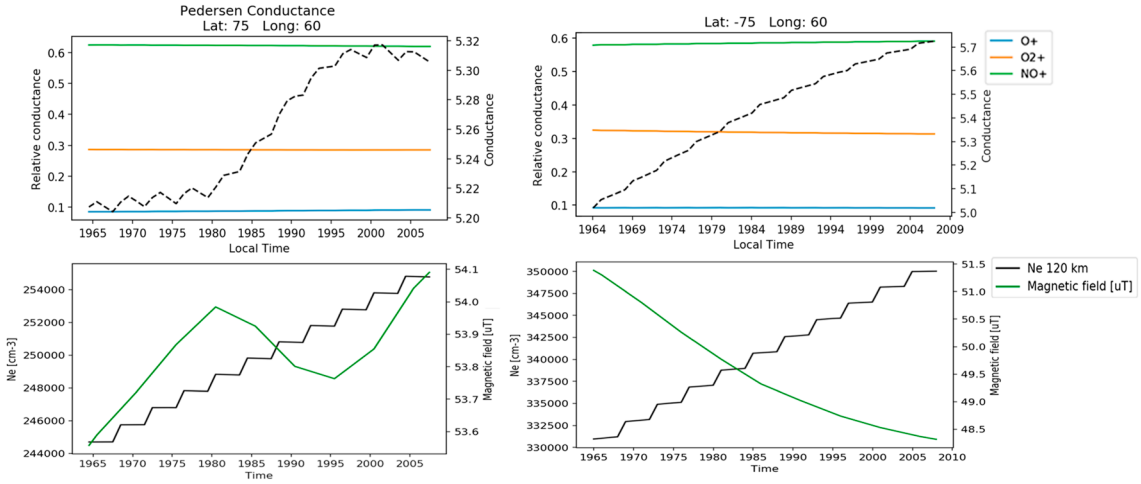

Figure 7. (top row) the Pedersen conductance in siemens (black dashed line) whit fixed low solar activity and ionic contribution (blue = O^+, green = NO^+, and orange = O_2^+) at polar locations (75°N 60°E and 75°S 60°E). (bottom row) The electron density at 120 km (black) and magnetic field intensity (green).

The daily variation at high latitudes, within the polar region, is presented in Figure 6 for the same equinoctial days of previous figures, low and high solar activity. During low activity levels NO^+ contribution to Σ_1 is around 60% during almost the whole day. However, Σ_1 is much lower than at middle latitudes. During daytime hours O_2^+ summed to NO^+ contribute ~90% of the total Pedersen conductance at the northern location. Only at night O^+ becomes the second main conductor. During periods of high solar activity O^+ takes again a big percentage of the conductance at nighttime hours. Note that the conductance is much lower during nighttime.

On the left column we can see that the conductance increases as the magnetic field does. Here, where conductance is low and magnetic field is strong, the electron density plays a more important role in conductance variability. It can be seen that the stronger conductance increase happens when the intensity of the magnetic field suffers a partial decrease around 1980–1995.

In the second location analyzed (bottom row) in Figure 7, Southern Hemisphere, the conductance increase is due to the electron density increment and the magnetic field decrease.

4. Conclusions

On average, higher conductance corresponds to higher relative contribution of O^+. The magnetic field intensity is a very important variable in Pedersen calculation. At the SAA zone, where the magnetic field intensity is lower than in other places, O^+ is almost always the main contributor to Pedersen conductance.

Near the magnetic poles, the field is strong enough to keep the major portion of conductance in the *E* layer, being NO^+ and O_2^+ responsible for ~90% of its value. However, for high solar activity, the *F* layer takes a nonnegligible percentage of the conductance.

Throughout a year the contribution of each ion to Pedersen conductance varies mainly according to solar radiation. Semiannual variation can be seen in Figure 2 at southern midlatitude location during solar maximum, determined by the O^+ behavior. Eastern location presents the regular annual variation, with summer values greater than winter with some evidence of a semiannual variation. The western location presents semiannual variation with some evidence of winter anomaly. Another important factor is the magnetic field intensity, giving more importance to NO^+ and O_2^+ closer to the poles and to O^+ near the weak magnetic field region (SAA).

The annual behavior also shows that not always the *E* layer is the main conducting layer, since at some seasons between 10% and ~60% of conductance take place in the upper layer and can be a big source of error if the upper level of integration for conductance assessment is considered below the *F* region.

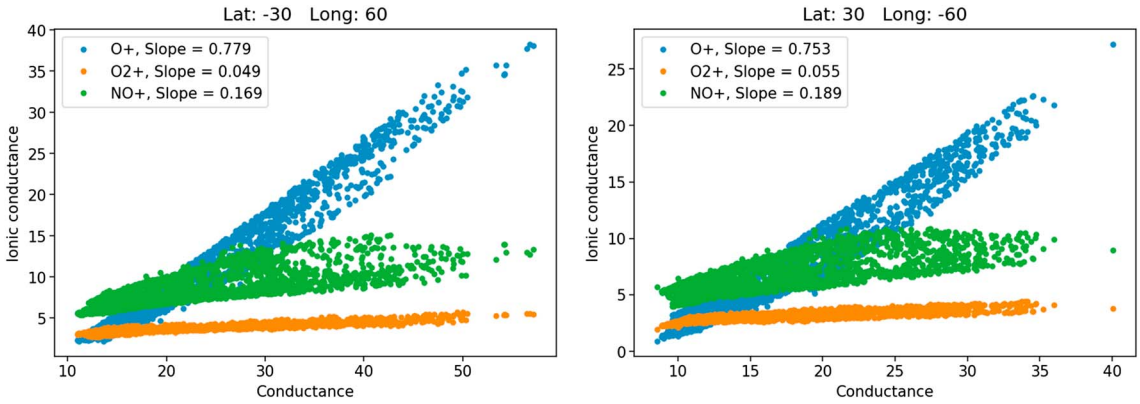

Figure 8. Ionic Pedersen conductance versus total Pedersen conductance in siemens. Points are calculated for 12 LT during days between 2001 and 2008 (not all point are plotted). Slope of each ion correspond to a first order linear regression.

The variations during the 44 years here considered, shown in Figure 3, indicate that O^+ conductance increase faster with solar activity than NO^+ and $O_2{}^+$. A kind of trend can be appreciated comparing the minimum periods of the solar cycle. However, we must be cautious considering that not all minima have exactly the same level of solar activity.

The trends for fixed solar activity and for a fixed date (Figures 4 and 7) show clearly the importance of magnetic field intensity in conductance long-term trend behavior. In the location of the left column of Figure 4 it is clear that conductance show an opposite behavior compared with the magnetic intensity at midlatitudes. When solar activity is forced to take low values, a difference is noticed and the electron density trend explains this.

Figure 5 shows how the magnetic field trend could be the bigger source of changes in the Pedersen conductance, at least at midlatitudes.

The analysis near the magnetic poles is a little more complex due to the Pedersen conductance take minimum values in these areas. Then trends of electron density and magnetic field have both a big impact over the conductance.

To resume, the behavior of each ionic contribution in terms of total conductance can be seen in Figure 8, at two different locations during the half solar cycle 2001–2008. From this figure it is clear that when Pedersen conductance increases, most of this increase is due to O+, which is the single ionic conductance with the greatest increasing rate.

Acknowledgments
We thank ISSI (International Space Science Institute, Bern) and ISSI-BJ (International Space Science Institute, Beijing) for their hospitality and support of the international team on "Climate Change in the Upper Atmosphere" where many ideas in this work were discussed. This work was supported by Projects PIUNT E642 and PICT 2015-C511. Data to calculate conductivities and Earth's magnetic field were freely obtained from IRI-2016 (http://omniweb.gsfc.nasa.gov/vitmo/iri2016_vitmo.html), NRLMSISE-00 (http://ccmc.gsfc.nasa.gov/modelweb/models/nrlmsise00.php), and IGRF (http://omniweb.gsfc.nasa.gov/vitmo/igrf_vitmo.html). This work can be replicated using pyglow, a Python package that wraps several upper atmosphere climatological models. The pyglow package is open sourced and available at the Github (https://github.com/tim-duly4/pyglow/). The model and simulations are also available from Bruno S. Zossi upon request (brunozossi@hot-mail.com).

References

Bilitza, D., Altadill, D., Zhang, Y., Mertens, C., Truhlik, V., Richards, P., et al. (2014). The International Reference Ionosphere 2012—A model of international collaboration. *Journal of Space Weather and Space Climate*, *4*, 1–12. https://doi.org/10.1051/swsc/2014004

Brekke, A., & Hall, C. (1988). Auroral ionospheric quiet summer time conductances. *Annales Geophysicae*, *6*, 361–376.

Cnossen, I., & Richmond, A. D. (2012). How changes in the tilt angle of the geomagnetic dipole affect the coupled magnetosphere-ionosphere-thermosphere system. *Journal of Geophysical Research*, *117*, A10317. https://doi.org/10.1029/2012JA018056

Cnossen, I., Richmond, A. D., & Wiltberger, M. (2012). The dependence of the coupled magnetosphere-ionosphere-thermosphere system on the Earth's magnetic dipole moment. *Journal of Geophysical Research*, *117*, A05302. https://doi.org/10.1029/2012JA017555

Cnossen, I., Richmond, A. D., Wiltberger, M., Wang, W., & Schmitt, P. (2011). The response of the coupled magnetosphere-ionosphere-thermosphere system to a 25% reduction in the dipole moment of the Earth's magnetic field. *Journal of Geophysical Research*, *116*, A12304. https://doi.org/10.1029/2011JA017063

Elias, A. G., Zossi, M., & de Haro Barbas, B. F. (2010). Trends in the solar quiet geomagnetic variation linked to the Earth's magnetic field secular variation and increasing concentration fo greenhouse gases. *Journal of Geophysical Research*, *115*, A08316. https://doi.org/10.1029/2009JA015136

High Altitude Observatory (2017). TIEGCM V1.94 Model description. National Center for Atmospheric Research, Boulder, CO. Retrieved from http://www.hao.ucar.edu/modeling/tgcm/doc/description/model_description.pdf

Moen, J., & Brekke, A. (1990). On the importance of ion composition to conductivities in the auroral ionosphere. *Journal of Geophysical Research*, *95*(A7), 10,687–10,693. https://doi.org/10.1029/JA095iA07p10687

Picone, J. M., Hedin, A. E., Drob, D. P., & Aikin, A. C. (2002). NRLMSISE-00 empirical model of the atmosphere: Statistical comparisons and scientific issues. *Journal of Geophysical Research*, *107*(A12), 1468. https://doi.org/10.1029/2002JA009430

Rasmussen, C. E., Schunk, R. W., & Wickwar, V. B. (1988). A photochemical equilibrium model for ionospheric conductivity. *Journal of Geophysical Research*, *93*(A9), 9831–9840. https://doi.org/10.1029/JA093iA09p09831

Rishbeth, H., & Garriott, O. K. (1969). *Introduction to ionospheric physics* (p. 334). New York: Academic Press.

Schunk, R. W., & Nagy, A. F. (2009). *Ionospheres: Physics, plasma physics, and chemistry*. New York: Cambridge University Press. https://doi.org/10.1017/CBO9780511635342

Sheng, C., Deng, Y., Lu, Y., & Yue, X. (2017). Dependence of Pedersen conductance in the *E* and *F* regions and their ratio on the solar and geomagnetic activities. *Space Weather*, *15*, 484–494. https://doi.org/10.1002/2016SW001486

Takeda, M., & Araki, T. (1985). Electric conductivity in the ionosphere and nocturnal ionospheric currents. *Journal of Atmospheric and Solar-Terrestrial Physics*, *47*(6), 601–609. https://doi.org/10.1016/0021-9169(85)90043-1

Thébault, E., Finlay, C. C., Beggan, C. D., Alken, P., Aubert, J., Barrois, O., et al. (2015). International Geomagnetic Reference Field: the 12th generation. *Earth, Planets and Space*, *67*(1), 79. https://doi.org/10.1186/s40623-015-0228-9

Zossi, B. S., Elias, A. G., & Fagre, M. (2018). Ionospheric conductance spatial distribution during geomagnetic field reversals. *Journal of Geophysical Research: Space Physics*, *123*, 2379–2397. https://doi.org/10.1002/2017JA024925

Zossi, B. S., Fagre, M., & Elias, A. G. (2018). On ionic contributions to Pedersen conductance. *Journal of Geophysical Research: Space Physics*, *123*, 10,310–10,318. https://doi.org/10.1029/2018JA026011